Journal of Nuclear Materials 382 (2008) 51–63

Contents lists available at ScienceDirect

Journal of Nuclear Materials

journal homepage: www.elsevier.com/locate/jnucmat

Hydrogen uptake of DPB getter pellets

L.N. Dinh [a,*], M.A. Schildbach [a], J.L. Herberg [a], A.P. Saab [a], J.C. Weigle [b], S.C. Chinn [a], R.S. Maxwell [a], W. McLean II [a]

[a] Lawrence Livermore National Laboratory, Livermore, CA, USA
[b] Los Alamos National Laboratory, Los Alamos, NM, USA

ARTICLE INFO

Article history:
Received 29 July 2008
Accepted 11 September 2008

ABSTRACT

The physical and chemical properties of 1,4-diphenylbutadiyne (DPB) blended with carbon-supported Pd (DPB–Pd/C) in the form of pellets during hydrogenation were investigated. A thermogravimetric analyzer (TGA) was employed to measure the kinetics of the hydrogen uptake by the DPB getter pellets. The kinetics obtained were then used to develop a semi-empirical model, based on gas diffusion into solids, to predict the performance of the getter pellets under various conditions. The accuracy of the prediction model was established by comparing the prediction models with independent experimental data on hydrogen pressure buildup in sealed systems containing DPB getter pellets and subjected to known rates of hydrogen input. The volatility of the hydrogenated DPB products and its effects on the hydrogen uptake kinetics were also analyzed.

Published by Elsevier B.V.

1. Introduction

Organic getters such as 1,4-diphenylbutadiyne (DPB) have a rapid and irreversible hydrogen uptake capability as well as a substantial hydrogen uptake capacity. The knowledge of the hydrogen uptake kinetics of such materials allows the prevention of hydrogen gas accumulation in sealed containers, which may lead to hydrogen corrosion of nuclear materials, undesirable effects on electronic components, or an explosion hazard [1–3]. However, there are only a few published studies on the kinetics of the gettering or scavenging of hydrogen by DPB getter [4–6]. In this report, the physical and chemical properties of DPB blended with carbon-supported Pd (DPB–Pd/C) in the form of pellets were examined. The hydrogen uptake kinetics of these getter pellets were obtained with a thermogravimetric analyzer (TGA) under isobaric, isothermal conditions. The kinetics obtained were then used to develop a semi-empirical model, based on gas diffusion into solids, to predict the hydrogen uptake performance of the getter pellets at lower hydrogen partial pressures conditions. The accuracy of this kinetic prediction model was established by comparing the predictive results with independent experimental data on hydrogen pressure buildup in sealed systems containing DPB getter pellets with known rates of hydrogen input. The volatility of the hydrogenated DPB products and its effect on the hydrogen uptake kinetics were also included in the prediction model. The unique approach to the hydrogen uptake kinetic measurement and prediction for DPB–Pd/C pellets as presented in this report serves to complement the meager current database on the efficiency of the DPB getter pellets during service life.

2. Experiments

2.1. Getter materials

In this report, the term 'virgin DPB' implies unreacted DPB while the term 'fully hydrogenated DPB' refers to 100% reacted DPB (also called 1,4-diphenylbutane). Some experiments were performed on commercial virgin DPB crystallites purchased from Aldrich Chemical Company, Inc., some others on fully hydrogenated DPB crystallites bought from Alfa Aesar, but most of the work was done with DPB pellets manufactured by the Kansas City Plant, Honeywell Federal Manufacturing and Technologies. These DPB pellets have a composition of 75 wt% DPB and 25 wt% catalyst (5 wt% Pd on activated carbon). The role of the nanometer scale Pd catalyst is to split molecular hydrogen into atomic hydrogen for DPB molecules, which do not interact with molecular hydrogen, to uptake. The activated carbon support has a very high specific surface area (1100 m^2/g) and serves to spread the Pd catalyst throughout the DPB pellet structure. The DPB pellets are right circular cylinders with a diameter of approximately 2.8 mm, height of 3.1 mm and an axial hole through the pellet with a diameter of about 0.89 mm. Both virgin and fully hydrogenated DPB crystallites are white. The dark color of the DPB pellet is simply the result of the presence of carbon.

2.2. Equilibrium vapor pressure measurement

To assess the volatility of DPB getter pellets during service, the equilibrium vapor pressures of commercial virgin DPB crystallites,

* Corresponding author. Tel.: +1 925 422 4271; fax: +1 925 423 8772.
E-mail address: dinh1@llnl.gov (L.N. Dinh).

0022-3115/$ - see front matter Published by Elsevier B.V.
doi:10.1016/j.jnucmat.2008.09.013

virgin DPB pellets and fully hydrogenated commercial DPB crystallites were measured by the technique of effusion thermogravimetry using a Cahn Versatherm vacuum microbalance with a base pressure in the range of 100–200 mPa. The Knudsen cells used in the effusion thermogravimetry were fashioned from gold foil with a thickness of 0.05 mm and had orifices ranging from 0.28 mm to 0.52 mm.

2.3. Hydrogen uptake kinetic measurement and testing of the kinetic prediction model

The kinetics of hydrogen uptake by DPB pellets were obtained under isothermal, isobaric conditions by recording the weight change with the Cahn Versatherm vacuum microbalance. Fig. 1 shows the chemical formulae for virgin DPB and fully hydrogenated DPB molecules. Each DPB molecule (molecular weight of 202 g/mol) can uptake a maximum of 8 hydrogen atoms. The reaction of DPB with atomic hydrogen is exothermic. But it was found experimentally, by embedding thermocouples into the different parts of the DPB pellets, that pseudo-isothermal condition (temperature fluctuation of less than 1 K) could be achieved if the experiments were carried out in one atmosphere of a premixed gas composed of 18% or less hydrogen with the balance being helium. The pseudo-isobaric condition for the experiment was achieved by connecting the Cahn microbalance to a large premixed H_2/He gas reservoir (approximately 0.2 m^3 total volume) such that the total amount of hydrogen consumption throughout the microbalance weight gain experiments (containing from 1 to 5 DPB pellets) was less than 0.1% of the initial H_2 inventory in the reservoir. For practical purposes, the DPB pellet experiments described above could be considered to have been carried out in an isothermal, isobaric condition. To take into account the volatility of hydrogenated DPB during hydrogen uptake, another set of experiments was performed in which the hydrogenation progress was deliberately stopped (by removing the H_2/He premixed gas and replacing it with pure He) at 5 wt%, 10 wt%, 20 wt%, etc. and the weight loss versus time (due to the volatility of the hydrogenated product) was measured.

A combination of the empirical kinetic data taken from the microbalance experiments and some common properties of all processes involving gas diffusion into solids formed the basis for kinetic predictions of hydrogen uptake under varying conditions and will be presented in detail in the next section. The accuracy of the predictive model was established by comparing the predictions with independent experimental data on hydrogen pressure buildup in sealed systems containing DPB getter pellets and subjected to known rates of hydrogen input. The hydrogen pressure buildup in these sealed containers was measured with MKS Baratron gauges (absolute pressure transducers) and the hydrogen input was fixed at some constant rate with the use of a MKS mass flow controller, which could be varied from 0.001 standard cubic centimeters per minute (sccm) to 0.2 sccm.

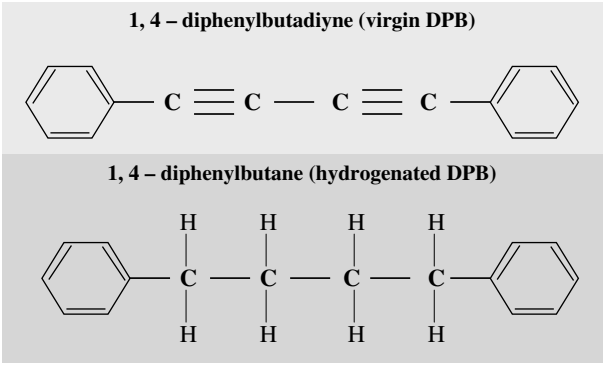

Fig. 1. The chemical formulae for virgin DPB and fully hydrogenated DPB.

2.4. Morphology and chemical identification

The morphologies of the DPB pellets as a function of hydrogenation levels were also probed with a commercial digital camera and a scanning electron microscope (SEM) in secondary electron mode. For all optical and SEM images, the samples were removed from the hydrogenation chamber and transported in laboratory air to the digital camera or SEM work station. The handling, transportation and even storage of the DPB getter pellets in air do not affect its performance.

To obtain chemical structure information, ^{1}H liquid state nuclear magnetic resonance (NMR) experiments were performed on a Bruker Advance 500 MHz spectrometer with a tunable broad band inverse (TBI) probe. All spectra were recorded at room temperature in CD_2Br_2.

3. Results

3.1. Equilibrium vapor pressures of virgin and fully hydrogenated DPB getters

The vapor pressure, P, is calculated from the rate of weight loss assuming effusive flow through the orifice of the Knudsen cell by the equation:

$$P = \frac{1}{[A.f]}\frac{dw}{dt}\sqrt{\frac{2\pi kT}{m}} \tag{1}$$

In Eq. (1), k is Boltzmann's constant, T is temperature, A is the orifice area, m is the mass of the vaporizing molecule, dw/dt is the mass rate of effusion and f is the Clausing factor [$f = 1 - 0.5(l/r) + 0.2(l/r)^2$ where l and r are the orifice length and radius, respectively]. Once a series of equilibrium vapor pressures at different temperatures was obtained, the enthalpy and entropy of vaporization (ΔH_{vap} and ΔS_{vap}) were derived from the Clausius–Clayperon Eq. (2)

$$\ln\left(\frac{P}{P_0}\right) = -\frac{\Delta H_{vap}}{RT} + \frac{\Delta S_{vap}}{R} \tag{2}$$

In Eq. (2), R is the molar gas constant and P_0 is the vapor pressure at boiling point (one atmosphere). A linear fit through the plot of $ln(P/P_0)$ vs. $1/T$ yields values of ΔH_{vap} and ΔS_{vap}. It can be observed from Fig. 2 that the vapor pressures of virgin DPB pellets were more scattered and somewhat lower than those of commercial virgin DPB crystallites. So, one effect of mixing the 25 wt% Pd/C catalyst with DPB was to effectively lower the vapor pressure of DPB in comparison with that of pure DPB crystallites. It is also seen from Fig. 2 that the vapor pressures of fully-hydrogenated DPB crystallites were significantly higher than those of their virgin counterparts. At 303 K, the equilibrium vapor pressure of fully hydrogenated DPB is close to 0.1 Pa, demonstrating that it is very volatile even at modest temperatures. Fig. 3 shows the plots of $ln(P/P_0)$ vs. $1/T$ for virgin DPB crystallites, virgin DPB pellets, and fully hydrogenated DPB crystallites. From this plot, the values of ΔH_{vap} and ΔS_{vap} were obtained and are presented in Table 1. From Table 1 and Eq. (2), it is clear that it is the combination of a low ΔH_{vap} value and a high ΔS_{vap} value that makes fully hydrogenated DPB more volatile than virgin DPB crystallites and virgin DPB pellets. Once ΔH_{vap} and ΔS_{vap} were obtained, Eq. (2) can also be used to calculate the equilibrium vapor pressure at any temperature.

The connection between the equilibrium vapor pressure of a material and its volatility can be seen from the Langmuir–Knudsen evaporation rate equation:

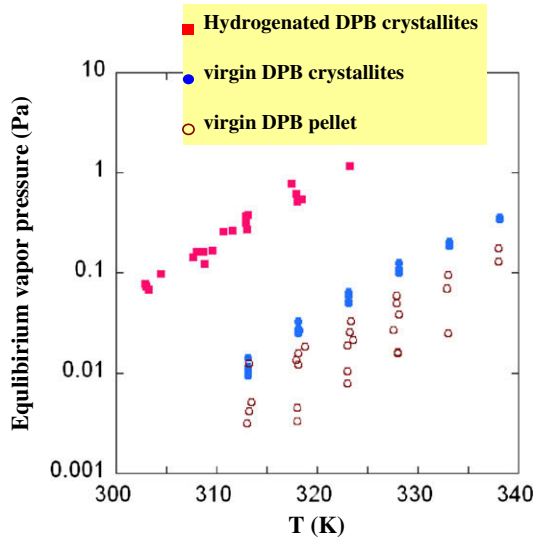

Fig. 2. The measured equilibrium vapor pressures of virgin DPB crystallites (solid circles), virgin DPB pellets with a formulation of 75 wt% DPB and 25 wt% Pd/C catalyst (open circles), and fully hydrogenated DPB crystallites (solid squares).

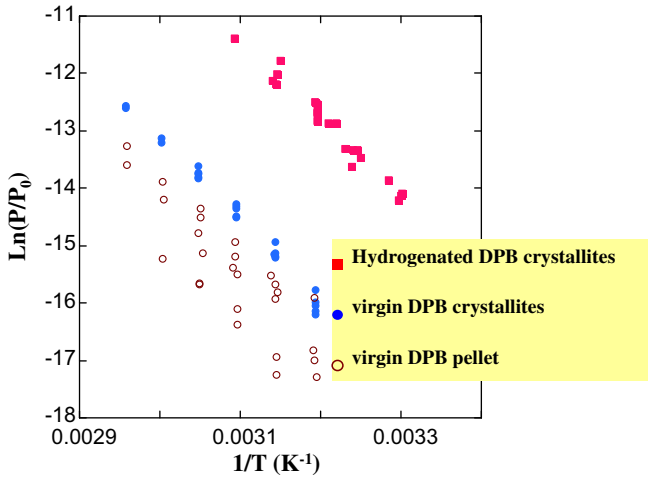

Fig. 3. The plot of $ln(P/P_0)$ vs. $1/T$ for virgin DPB crystallites (solid circles), virgin DPB pellets with a formulation of 75 wt% DPB and 25 wt% Pd/C catalyst (open circles), and fully hydrogenated DPB crystallites (solid squares).

Table 1
Enthalpy and entropy of vaporization for the different types of DPB under study

	Virgin DPB crystallites	Virgin DPB pellets (75 wt% DPB and 25 wt% Pd-C)	Hydrogenated DPB crystallites
ΔH_{vap} (kJ/mol)	111	122	113
ΔS_{vap} (kJ/mol)	0.22	0.26	0.26

$$J_v = \sigma \frac{(P_{equi} - P_a)}{\sqrt{2\pi mkT}} \quad (3)$$

In Eq. (3), J_v is the net vaporization flux in molecules per unit area per unit time, σ is the vaporization coefficient which depends on the material under study and its surface finish, while P_{equi} and P_a are the equilibrium and actual vapor pressures, respectively, over the evaporating surface. From Eq. (3), it is expected that a product with a high equilibrium vapor pressure suffers significant weight loss due to the vaporization of its molecules at the surface into the surrounding environment. Consequently, the study of the kinetics of hydrogen uptake of DPB through weight gain measurements must take into account the weight loss due to the high volatility of the hydrogenated product.

From this point on, the report is concerned only with the DPB pellets (75 wt% DPB + 25 wt% Pd/C catalyst).

3.2. Morphological changes of the DPB getter pellets with hydrogenation and associated chemical identification

SEM images of virgin and partially reacted DPB pellets at different magnification levels are shown in Figs. 4 and 5. The inset of Fig. 4 shows an optical image of virgin DPB pellets. The pellets were solid with the dimensions described in the experimental section. The bottom two SEM images show the morphology at the outer surface of the virgin DPB pellets. The top two SEM images reveal the porosity in the structure of the DPB pellets as observed from the cross-section of a DPB pellet which was broken in half. Note that the porosity observed in the broken virgin DPB pellet is closed, not an open porosity structure for gas molecules to move through as in the case of a sponge. The left column in Fig. 5 presents SEM images at the outer surface of a DPB pellet at ~25 wt% hydrogenation, while the right column in Fig. 5 contains the optical images of another DPB pellet at ~75 wt% hydrogenation. Clearly, at high hydrogenation levels, the pellet had softened considerably. The washout spot near the middle of the upper left SEM image in Fig. 5 was an artifact formed when the electron beam in the SEM was focused on that spot of the roughly 25 wt% hydrogenated DPB pellet. This pellet also looked partially liquefied, albeit not to the drastic level seen at 75 wt% hydrogenation. In fact, all DPB pellets that have been hydrogenated to beyond a few weight percent exhibited increasing level of liquefaction with further hydrogenation, even when observed by eye.

^{1}H NMR investigations revealed the existence of four different hydrogen configurations in a ~52% hydrogenated DPB pellet sample, including a fully hydrogenated state and three partially hydrogenated states. All of the ^{1}H NMR configurations are shown in Fig. 6. In this figure, the peaks at ~7.5 ppm (part per million in the NMR context represents a chemical shift defined by dividing the frequency shift by the applied frequency, then multiplying by 10^6) and ~7.6 ppm are ^{1}H NMR associated with the aromatic protons on the phenyl ring of the DPB molecules. The peaks at 1.9 ppm and 2.9 ppm are ^{1}H NMR associated with aliphatic protons (CH_2) attached to the phenyl rings in the fully hydrogenated DPB structure. The doublets near 3.7 ppm and 6 ppm are associated with the protons in the CH groups belonging to partially hydrogenated DPB molecules containing 6 hydrogen atoms. The doublets near 6.7 ppm, and 6.9 ppm are associated with the protons in CH groups belonging to partially hydrogenated DPB molecules containing 4 hydrogen atoms. Partially hydrogenated DPB molecules with only two hydrogen atoms produce only a ^{1}H NMR doublet at ~6 ppm. The peak at ~5.3 ppm is from the ^{1}H NMR of CD_2Br_2 solvent. Thus, partially hydrogenated DPB pellets show the presence of partially and fully hydrogenated DPB molecules. One hypothesis is that the partially hydrogenated products form a eutectic with unreacted DPB. Unfortunately, the effect of how chemical changes might induce the liquefaction of partially hydrogenated DPB pellets, while a subject of some interest, is beyond the scope of this work.

The top right image in Fig. 7 is a digital camera image of fully hydrogenated DPB pellets which were the result of leaving these pellets in a closed chamber with roughly 6000 Pa of hydrogen for a few weeks. The rest of Fig. 7 represents SEM images of fully hydrogenated DPB pellets at different magnification levels. Fully hydrogenated DPB pellets are solid, just as the 100% reacted DPB crystallites obtained commercially from Alfa Aesar. However,

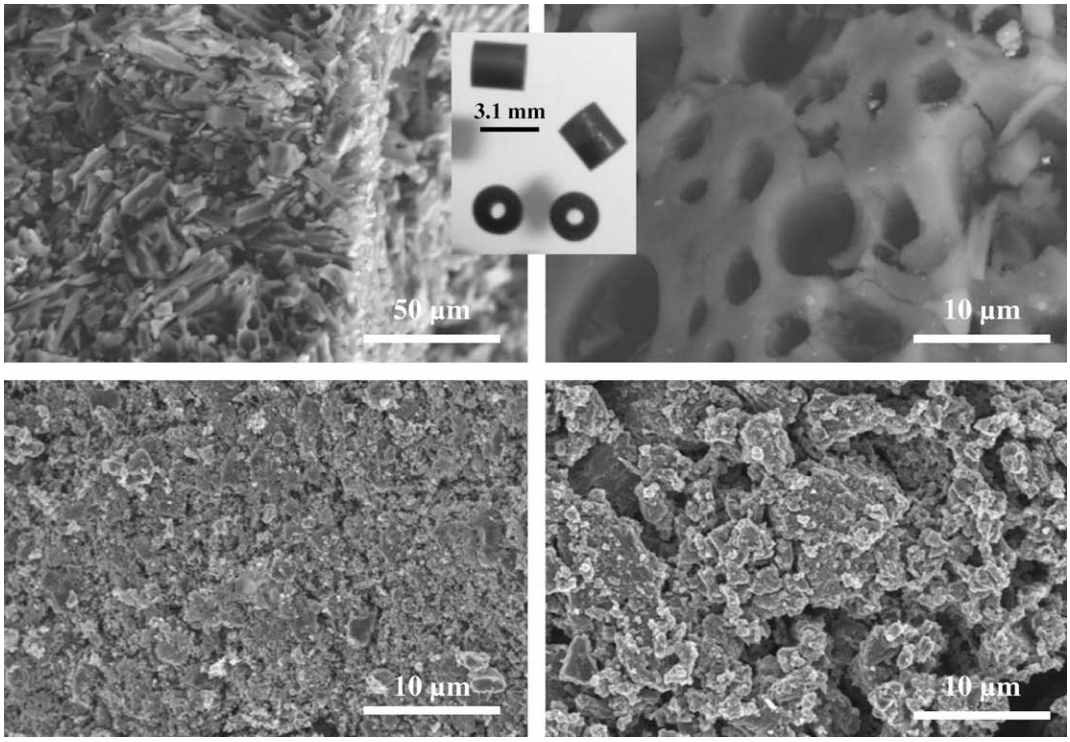

Fig. 4. SEM images of virgin DPB pellets at different magnification levels. The inset is an optical image of a few virgin DPB pellets. The bottom two SEM images show the morphology at the outer surface of the virgin DPB pellets while the top two SEM images reveal the porosity (closed structure, not open porosity) of a fracture surface.

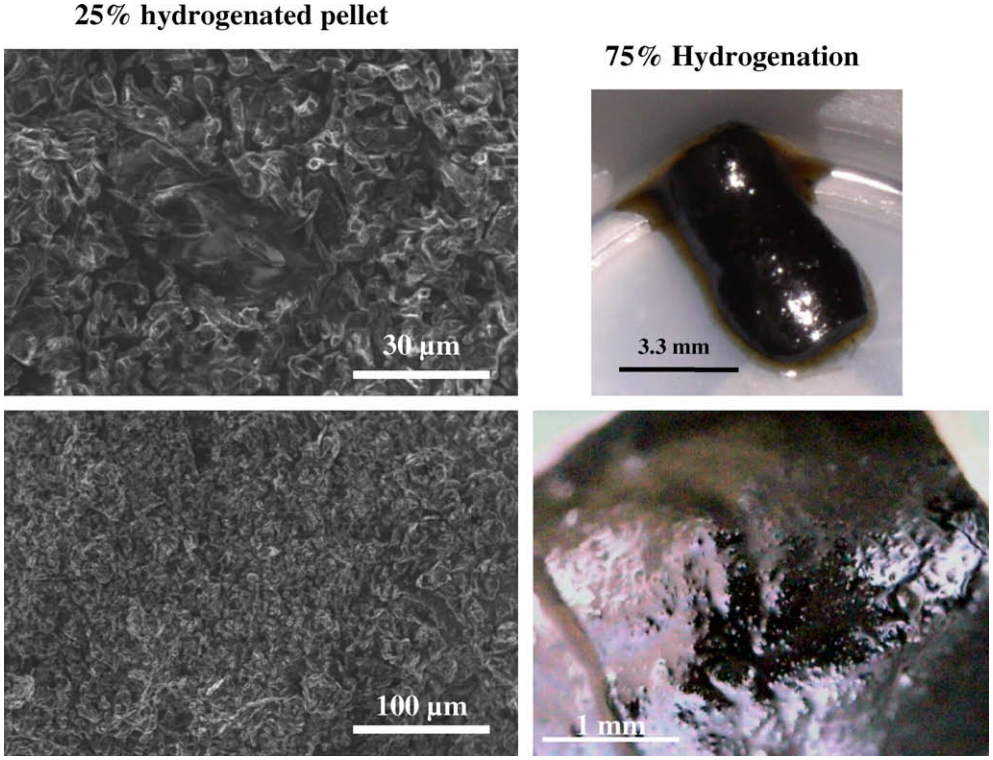

Fig. 5. The left column presents SEM images at the outer surface of a DPB pellet at around 25 wt% hydrogenation at different magnification levels, while the right column contains the optical images of another DPB pellet at around 75 wt% hydrogenation.

unlike the virgin DPB pellets, the fully hydrogenated DPB pellets were friable upon being touched. Most fully hydrogenated DPB pellets had elongated or squashed shapes. Many even fused together where they touched. Clearly, in going from the virgin state to fully hydrogenated state, the DPB pellets have gone through some dramatic changes which would be expected to result in a constantly changing vaporization coefficient σ in the Langmuir–Knudsen evaporation rate Eq. (3).

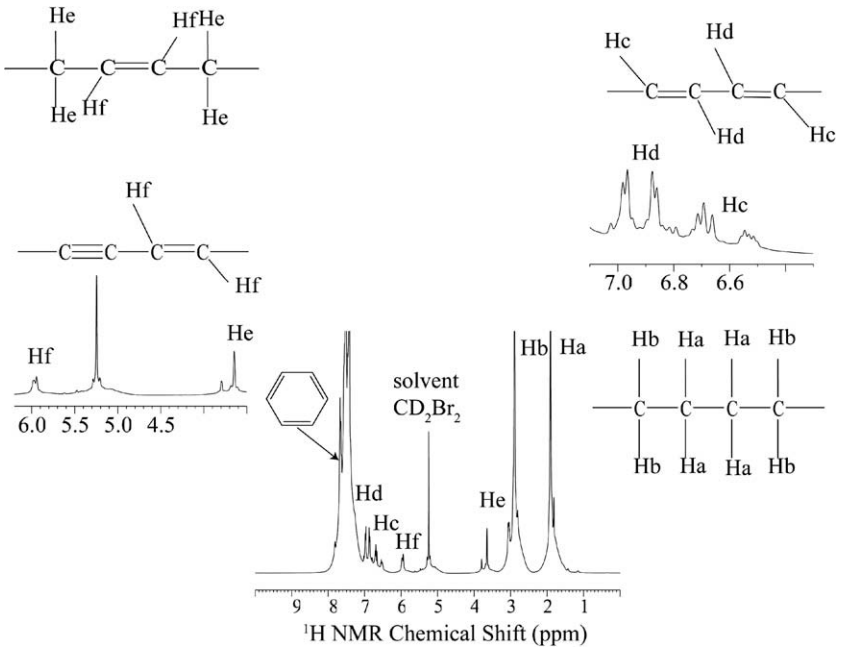

Fig. 6. NMR investigation of the chemical structure of partially hydrogenated DPB.

3.3. Hydrogen uptake kinetics of DPB getter pellets

All these complexities make the quantification of the weight loss of hydrogenated DPB pellets as a function of hydrogenation level using the Langmuir–Knudsen formulation in Eq. (3) impractical. Instead, the weight loss was measured directly as a function of hydrogenation level. In a series of microbalance experiments, a H_2/He gas mixture was used to bring DPB pellets to certain predetermined hydrogenation levels (e.g. 5 wt%, 10 wt%, 20 wt%, etc.). At this moment, the reaction was halted by pumping out the H_2/He gas and replacing it with pure He. The weight loss versus time due to the volatility of the hydrogenated product was then measured during the first few minutes after the microbalance had recovered from the perturbation of the gas change. In Fig. 8, a plot of the weight loss rate of hydrogenated DPB pellets as a function of the apparent hydrogenation percentage (before correction for product volatility) at ~294 K as recorded by the TGA is presented. From this plot, it is observed that the volatility of the hydrogenated

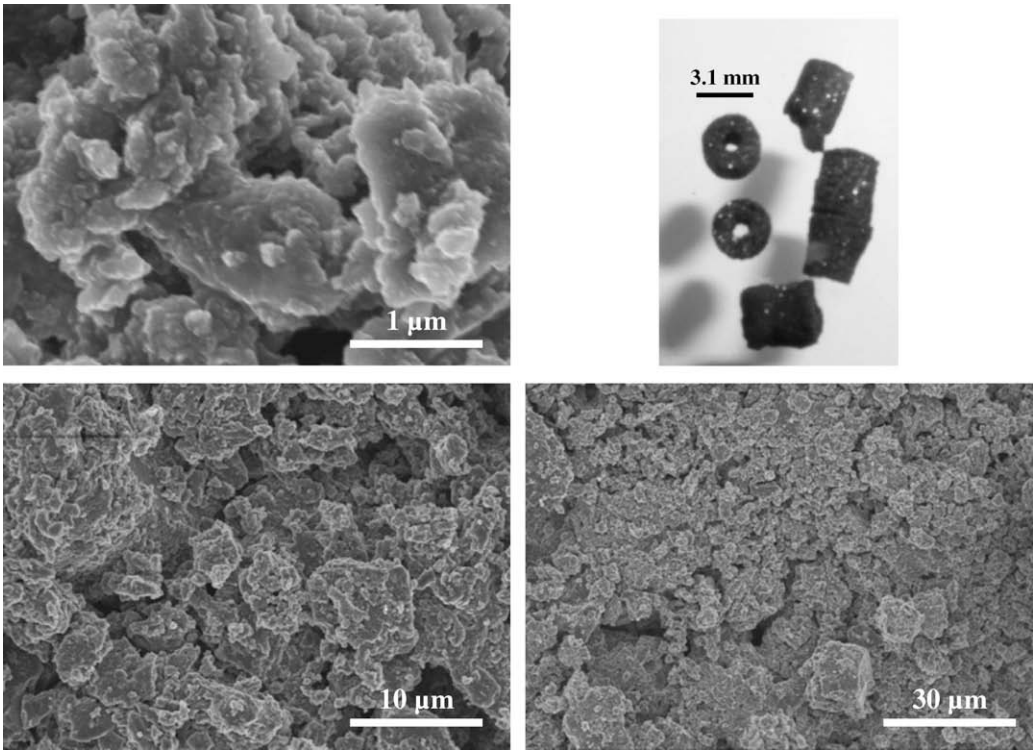

Fig. 7. Optical (top right corner) and SEM (the rest) images of fully hydrogenated DPB pellets.

DPB pellets increases with increasing level of hydrogenation up to around 20% hydrogenation level, after which the degree of volatility decreases.

This observation is in qualitative agreement with the morphology changes seen during the process of hydrogenation of the DPB pellets presented in Figs. 4–7 for the following reasons. As the hydrogenation process went on, the rate of weight loss increased due to the formation of the more volatile hydrogenated product. As the DPB pellets got hydrogenated further, they also became more liquefied. At around 20% hydrogenation level, the liquefaction must have progressed enough to effectively reduce the surface area available for vaporization of the hydrogenated product resulting in a decrease in the rate of weight loss. At ~65% hydrogenation level, the liquefaction apparently reached a saturation level, and the rate of weight loss was roughly constant thereafter. It is noted that the difference in the rates of weight loss due to the volatility of virgin DPB pellets and the highly hydrogenated DPB pellets (Fig. 8) is not quite the same as the difference in the equilibrium vapor pressures measured for virgin DPB crystallites and fully hydrogenated DPB crystallites (Fig. 2). This was probably due to changes in the porosity structure, grain sizes, and surface area available for vaporization of the DPB pellets in going through liquefaction during the hydrogenation process and re-solidification near the completion of this process. The observed error bar associated with the data points in Fig. 8 was ~35% and was due to a combination of pellet to pellet variation and experimental variability.

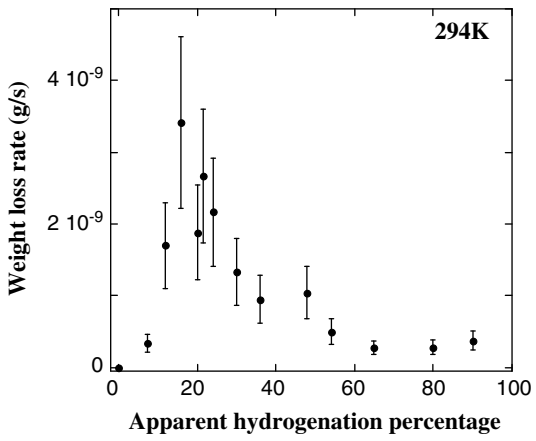

Fig. 8. A plot of the weight loss rate of hydrogenated DPB pellets as a function of the apparent hydrogenation percentage at room temperature (294 K) as recorded by the TGA.

Figs. 9(a) and (b) show the plots of the hydrogenation percentage vs. time and the hydrogen uptake rate per pellet vs. corrected hydrogenation percentage curve for typical isobaric, isothermal hydrogen uptake experiments with DPB pellets at 294 K. The gas used in this experiment had a total pressure of one atmosphere and was composed of 10% hydrogen with the balance being helium. In Fig. 9(a), the dashed and solid curves represent the hydrogenation vs. time curves prior to and after the correction for weight loss due to the volatility of the hydrogenated products, respectively. The correction for weight loss due to the volatility of the hydrogenated products was achieved by adding the weight loss as a function of hydrogenation level to the apparent weight gain curves due to hydrogen uptake. The weight loss due to the volatility of the hydrogenated product ceases when the equilibrium vapor pressure of the reacted product is reached within the reaction vessel. So, corrections for the volatile nature of the reacted product should be much smaller in closed systems with smaller volumes.

The hydrogenation percentage vs. time curve presented in Fig. 9(a) displays fairly abrupt changes at around 40% and 85%. The hydrogen uptake rate per pellet vs. corrected hydrogenation percentage curve in Fig. 9(b) shows even more abrupt rate changes at around 10%, 40% and 85%. The performance of the DPB getter reached its lowest level beyond 60% consumed capacity, but increased again around 85%. This increase in performance is attributed to the onset of the re-solidification of heavily hydrogenated DPB molecules on the high surface area of the carbon support. This phenomenon causes an increase in the surface area available for H_2 adsorption as well as for vaporization of hydrogenated products, resulting in a jump of the hydrogen gettering rate near the end of life of the DPB pellets.

Obviously, the hydrogenation process of the DPB pellets is very complex and the kinetics of the hydrogen uptake of the DPB pellets, therefore, cannot be accurately described by a single stage geometrical diffusion model with a constant diffusion coefficient and a single activation energy. Consideration of the hydrogen uptake process by the DPB pellets at the atomic scale also leads to many questions and few answers (Fig. 10). The cartoon on the right-hand side of Fig. 10 depicts an exploded view of a Pd catalyst inside a DPB pellet. Each hydrogen molecule is split into two hydrogen atoms upon adsorbing on the Pd catalyst surface. These hydrogen atoms react readily with DPB molecules that touch the surface of the Pd catalyst to form a product layer of hydrogenated

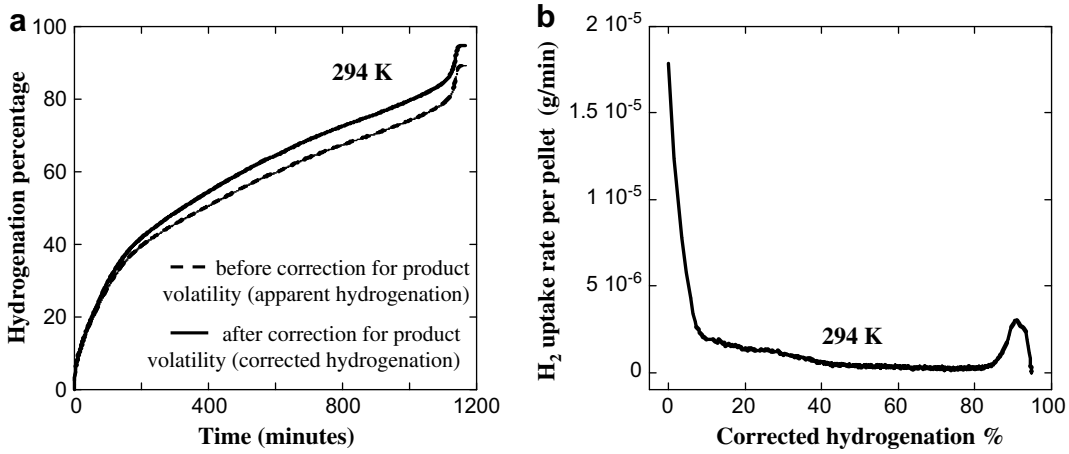

Fig. 9. The hydrogenation percentage vs. time curve (a) and the weight gain rate per pellet vs. corrected hydrogenation percentage curve (b) for a typical experiment with DPB pellets at 294 K in an isobaric environment of one atmosphere (10% H_2 + 90% He) are presented.

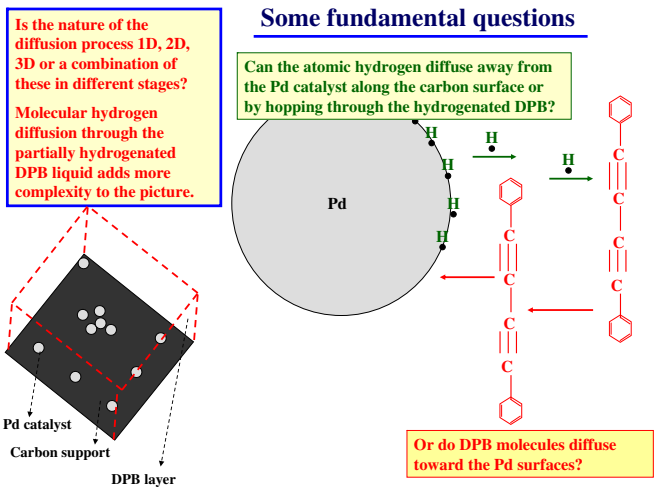

Fig. 10. Cartoons illustrating the complexity involved in the uptake of hydrogen by DPB pellets at the microscopic and/or atomic levels.

DPB. After the formation of this product layer, between the Pd catalyst surface and virgin DPB, how does the reaction continue? Would hydrogen leave the Pd catalyst surface and diffuse as atomic hydrogen through the thickening layer of hydrogenated DPB product to continue the reaction? Computational modeling suggests that the energy of direct desorption of a hydrogen radical from the Pd surface is prohibitively large, ~254 kJ/mol [7]. However, there is experimental evidence in the literature to support the diffusion of atomic hydrogen on macroscopic scale away from the Pd catalyst surface when the Pd catalysts sit on a graphite substrate [8]. In the case of DPB pellets, the Pd catalysts are on an activated carbon support which is not graphitic in nature but more like amorphous carbon. Amorphous carbon does contain isolated local graphitic domains, but does not have a graphitic structure on a large scale. So, the ability of hydrogen atoms to leave the Pd catalyst sites to react with DPB molecules at far distance is greatly questionable in the DPB pellet structure. There is, however, a possibility that hydrogen radicals can hop through the hydrogen bonds in the hydrogenated DPB structures to react with far away DPB molecules, but a thorough study on this subject is still lacking in the literature [7]. In addition, the solubility of hydrogen in Pd increases with hydrogen pressure and the Pd catalysts are certainly expected to exist as palladium hydride under the experimental conditions described in this report (one atmosphere of $\geqslant$10% hydrogen in helium), so can the catalysts also act as a reservoir for supplying hydrogen to surface sites? The catalysts undoubtedly serve as local reservoirs for supplying hydrogen to surface sites in a gas-burette setup in which the hydrogen pressure in the environment surrounding the catalysts decreases with time [4]. But in isobaric experiments or a dynamic application in which the hydrogen pressure remains unchanged or increases with time such as those considered in this report, the hydrogen solubility in the catalysts has to remain constant or increases with time. Consequently, the catalysts cannot act as local suppliers of hydrogen to surface sites in such conditions. Another question is whether the DPB molecules far away from the Pd catalysts can diffuse toward the Pd surface to capture hydrogen radicals. This is a real possibility given the liquid like nature of the DPB pellets during much of the hydrogenation process (see Fig. 5). All of these proposed mechanisms involve diffusion, raising the question of whether the diffusing species (hydrogen radicals and/or DPB molecules) strictly follows a one, two or three dimensional diffusion profile. The left-hand side cartoon in Fig. 10 illustrates this point. The DPB pellet contains 25 wt% catalyst (5 wt% Pd on carbon support). Since the average size of the Pd catalyst particle is on the order of nanometer scale, the average inter-particle distance is on the order of a few micrometers. The average thickness of the DPB layer on top of this structure of scattered Pd particles on carbon is also on the order of a few micrometers. The initial diffusion of hydrogen radicals away from the Pd surface (if at all possible) along the carbon surface have a two dimensional nature (actually three dimensional nature if the curvature of the carbon surface is taken into account). The diffusion of DPB molecules toward the Pd catalysts should have a three dimensional nature in the vicinity of the catalyst. A few micrometers away from the nanometer-scale Pd catalysts, the diffusion of DPB molecules toward the Pd should be more or less one dimensional in nature. At high levels of hydrogenation (images in the right column of Fig. 5), the diffusion of molecular hydrogen through the partially hydrogenated DPB liquid to reach the Pd catalysts only adds more complexity to the picture.

3.4. A semi-empirical model for the hydrogen uptake of DPB getter pellets

In order to circumvent the difficulties associated with what would be a very complicated atomistic or microscopic model, a semi-empirical kinetic model based on the general properties of gaseous diffusion into a solid (or liquid) was instead developed. A general property of all isothermal, isobaric processes in which the diffusion and incorporation of a gas into a solid (or liquid) is the rate limiting step can be written mathematically as

$$P_1 t_1 = P_2 t_2 \quad \text{for} \quad T_1 = T_2 = T \tag{4}$$

The mathematical proof of Eq. (4) can be found in Appendix A. The implication of Eq. (4) is that if it takes a time t_1 at a constant pressure P_1 to reach a certain conversion level (hydrogenation percentage or weight gain as in the case of this report), then it takes a time t_2 at a constant but lower pressure P_2 to reach the same conversion level such that t_2 can be deduced from t_1, P_1 and P_2, given that the temperature T_1 in the experiment with pressure P_1 is the same as the temperature T_2 in the experiment with pressure P_2. Previously reported experiments with hydrogen uptake in 1, 4-bis(phenylethynyl)benzene, also called DEB, mixed with carbon-supported Pd in a slab geometry confirmed that the diffusion of molecular hydrogen through the hydrogenated product layer to the virgin DEB compound material inside as the rate limiting step for the process [3]. Despite their different chemical formulae and physical properties (higher melting point and lower vapor pressure for DEB), DPB and DEB are in the same family of organic hydrogen getters, and the percentage of carbon-supported Pd catalyst in the DEB compound is the same as that for the DPB pellets. It is, therefore, expected that the diffusion of molecular hydrogen through the hydrogenated product layer to the virgin DPB sites is also the rate limiting step for hydrogen uptake process in DPB pellets and that Eq. (4) is applicable.

In Fig. 11(a), the scatter in the maximum gettering capacities (or maximum hydrogenation percentage after correction for product volatility) of 10 DPB pellets is presented. Even though the average composition of DPB pellets is 75 wt% DPB and 25 wt% catalyst (5 wt% Pd on carbon support), the composition of individual DPB pellets vary somewhat from the nominal composition. Consequently, the observed scatter in the maximum gettering capacities of these 10 DPB pellets is likely a combination of variation in individual pellet composition and experimental variability. In Fig. 11(b), the gray shadow represents the prediction of what the plot of hydrogenation percentage vs. time curve is expected to look like for an isothermal (294 K) isobaric (10% H_2 + 90% He at one atmosphere) hydrogen uptake experiment by DPB pellets based on relationship (4) and the experimental data obtained using a gas mixture of 18% H_2 + 82% He at one atmosphere. The spread in

the time scale (~35% error bar) of the gray shadow represents the typical scatter in experimental data obtained under similar conditions due to the non-uniformity of the pellets. The two dark solid lines in Fig. 11(b) are actual plots of the hydrogenation percentage vs. time for two experiments carried out in an isothermal (294 K), isobaric (10% H_2 + 90% He at one atmosphere) environment. Fig. 11(b) suggests that, within the observed scatter in data, hydrogen uptake data obtained at a higher hydrogen partial pressure (shorter experimental time) can be used to predict a hydrogen uptake process at a lower hydrogen partial pressure using Eq. (4), provided that the temperature in the high pressure experiment is the same as that intended for the low pressure prediction.

In general, the hydrogen partial pressure in a real device is not constant over a long period of time. However, if the unit of time is chosen to be very small, such as one second, then during each one second time interval, the condition of constant pressure can be practically assumed and the use of Eq. (4) during that one second time interval is justified. The net hydrogen partial pressure in a device as a function of time can then be predicted numerically using:

$$P(t,\alpha) = P(t-\Delta t,\alpha-\Delta\alpha) + P'_D(t)\Delta t - \left(\frac{NRT}{VM_{H_2}}\right) \times \left\{\frac{P(t-\Delta t,\alpha-\Delta\alpha)}{P_E}W'_E(\alpha) - \left[W'_L(\alpha)\frac{P_{equi}(T)}{P_{equi}(294K)}\right] \quad \frac{P_{equi}(T)-P_a(t-\Delta t,\alpha-\Delta\alpha)}{P_{equi}(T)}\right\}\Delta t \tag{5}$$

The derivation of Eq. (5) is found in Appendix B. In Eq. (5), $P(t, \alpha)$ is the net hydrogen pressure in the device at time t. Note that P is a function of both time and the average hydrogenation percentage or consumption level of the DPB getter pellets, α. $P(t-\Delta t, \alpha-\Delta\alpha)$ is the net hydrogen partial pressure in the device at time $(t-\Delta t)$ when the consumption level of the DPB pellet is $\alpha-\Delta\alpha$. In this work, Eq. (5) is solved numerically with a Fortran program and Δt is taken to be one second. $P'_D(t)$ is the rate of hydrogen pressure increase, generated by all processes inside the device without any DPB getter, at time t. For the situations considered here, P_D is strictly a constant or only a function of time. The third term on the right-hand side of Eq. (5) represents the rate of hydrogen pressure decrease due to the scavenging action of the DPB getter pellets. Here, N, R, V and M_{H_2} stand for the number of DPB pellets employed in the device, molar gas constant, the free volume of the device, and molecular weight of hydrogen (2 g/mol), respectively. P_E is the hydrogen partial pressure employed in the isothermal, isobaric experiment at higher pressure to obtain the plot of the H_2 uptake rate of one DPB getter pellet vs. the percentage hydrogenation, $W'_E(\alpha)$ (see Fig. 9(b) at T = 294 K). $W'_L(\alpha)$ is the experimentally obtained rate of weight loss of just one DPB pellet as a function of α at 294 K (see Fig. 8), $P_{equi}(T)$ is the equilibrium vapor pressure of the hydrogenated product at temperature T, and $P_a(t-\Delta t, \alpha-\Delta\alpha)$ is the actual vapor pressure of the hydrogenated product in the device at time $t-\Delta t$ and hydrogenation level $\alpha-\Delta\alpha$. At any given temperature, the performance of the DPB getter pellets, as described by Eq. (5), depends on the consumed getter capacity level, the instantaneous hydrogen partial pressure, the number of DPB getter pellets, and the free volume of the device. Since P_E, $W'_E(\alpha)$, and $W'_L(\alpha)$ were experimentally obtained, the hydrogen pressure buildup prediction Eq. (5) is semi-empirical in nature.

The use of Eq. (5) to obtain the hydrogen partial pressure evolution in a device is illustrated in Fig. 12. In Fig. 12(a), the experimentally measured hydrogen pressure buildup vs. time curve for a vessel having a free volume of 700 cc (or cubic centimeters), containing 20 DPB pellets at 294 K and subjected to a constant hydrogen input rate of 0.043 sccm is presented by the dark solid line. The light dashed line in the same figure represents the linear hydrogen pressure buildup curve resulting from a constant hydrogen input rate of 0.043 sccm in the same vessel under the same situation, but without any DPB getter pellet inside. Also in the same figure, the dark dashed line is the predictive modeling of what the hydrogen pressure buildup in the system is expected to look like from the use of Eq. (5) and isothermal isobaric data at higher hydrogen partial pressure presented in Fig. 9(b). Fig. 12(b) shows a similar situation to that in Fig. 12(a) but with a vessel having a free volume of only 522.3 cc and a constant hydrogen input rate of 0.034 sccm. The discrepancy between the semi-kinetic prediction model and experimental hydrogen pressure buildup data is attributed to the non-uniformity of the DPB pellets and experimental variability in both the hydrogen pressure buildup experiments and the weight change experimental data employed in the semi-kinetic prediction model. From Fig. 12, it is observed that the DPB getter pellets' performance continually drops with increasing consumed capacity as expected for a gas–solid diffusion process. However, near the end life of the DPB getter pellets, a surge in the hydrogen gettering rate due to the re-solidification of the heavily hydrogenated DPB molecules on the high surface area carbon support (see Fig. 9(b) at $\geqslant$85% hydrogenation level) causes the hydrogen pressure buildup in the device to drop significantly until very near the end of life of

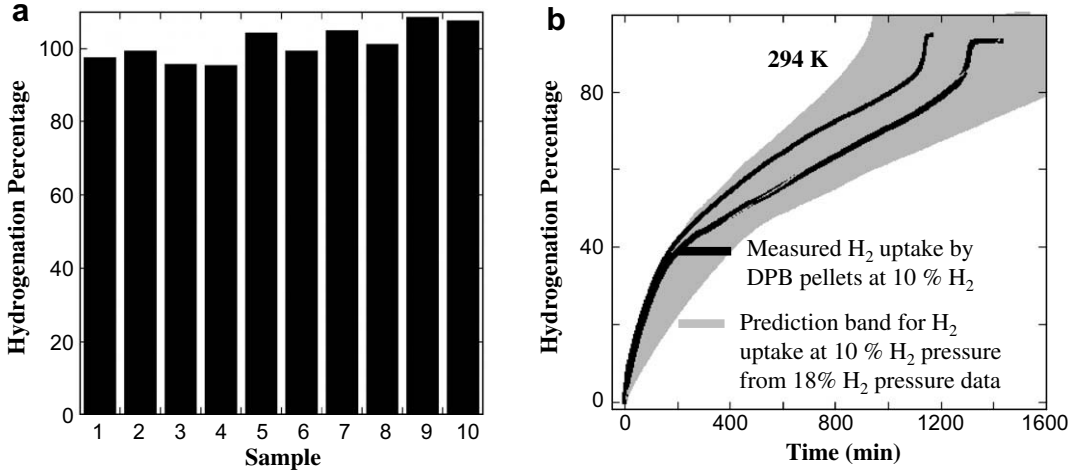

Fig. 11. (a) the scatter in the maximum gettering capacities of 10 DPB pellets due to sample to sample variation in composition and (b) the level of agreement between actual isothermal, isobaric hydrogen uptake data at a H_2 partial pressure of 10133 Pa and predicted uptake at 10133 Pa from data at a H_2 partial pressure of 18239 Pa at 294 K.

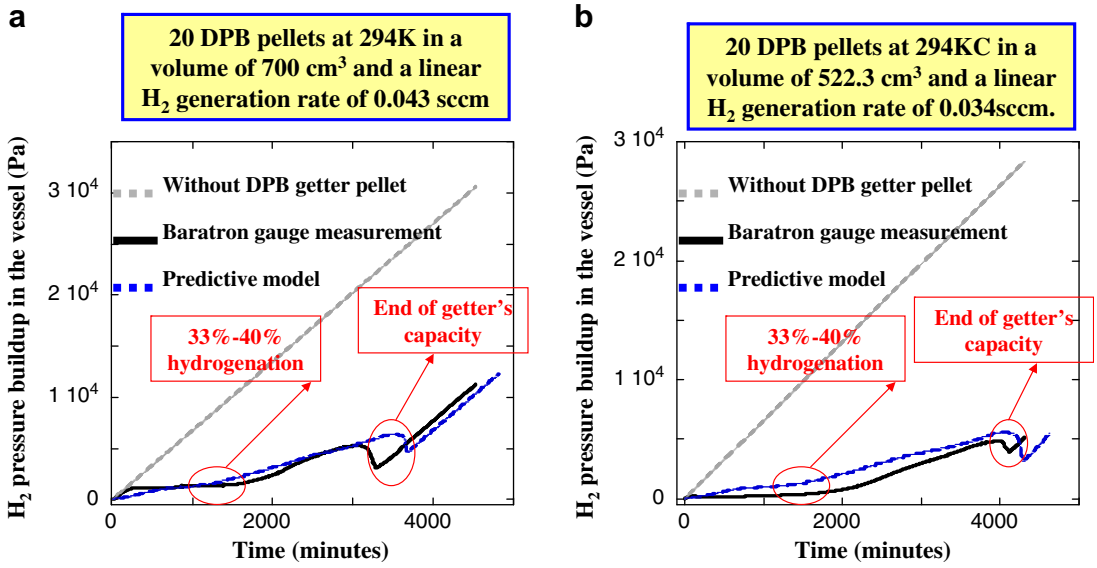

Fig. 12. Hydrogen pressure buildup without DPB getter pellets (light dashed lines) and with 20 DPB getter pellets (dark solid lines) at 294 K under a constant hydrogen input rate of 0.043 sccm in a 700 cc vacuum vessel (a) and under a constant hydrogen input rate of 0.034 sccm in a 522.3 cc vacuum vessel (b). The dark dashed lines represent the hydrogen pressure rise as predicted by the semi-empirical kinetic predictive models described in Eq. (5).

the getter pellets. From that point on, the hydrogen pressure rise in the device is solely a function of the hydrogen input rate, which is linear in this report.

Fig. 13(a) shows the plot of the hydrogen uptake rate per pellet vs. corrected hydrogenation percentage curve for typical isobaric, isothermal hydrogen uptake experiments for DPB pellets at 303 K. The gas used in this experiment was fixed at 10% H_2 and 90% He with a total pressure of one atmosphere. Analogous to Fig. 12, in Fig. 13(b), the experimentally measured hydrogen pressure buildup vs. time curve for a vessel having a free volume of 466.5 cc, containing 10 DPB pellets at 303 K and subjected to a constant hydrogen input rate of 0.027 sccm is presented by the dark solid line. The light dashed line represents the linear hydrogen pressure buildup curve resulting from a constant hydrogen input rate of 0.027 sccm in the same vessel without any DPB getter pellet. The dark dashed line in Fig. 13(b) represents the predictive modeling of what the hydrogen pressure buildup in the system is expected to look like from the use of Eq. (5) and the weight gain rate per pellet vs. corrected hydrogenation level curve obtained in an isothermal, isobaric experiment at high hydrogen pressure (Fig. 13(a)). In general, the DPB getter pellets lose their effectiveness as their capacity decreases (evidenced by the increase in the hydrogen pressure buildup with time). This is qualitatively expected for all reactions involving the diffusion of gas molecules through a constantly increasing product layer. The dramatic drop in hydrogen pressure near the end of life of DPB pellets at 294 K (as observed in Fig. 12) was, however, not present at 303 K (see Fig. 13). This drop in the hydrogen pressure in the device near the end of life of the DPB getter pellets was attributed to the re-solidification of the getter pellets at a high hydrogenation percentage from a liquid like state at 294 K as described earlier on. The re-solidification of the DPB getter pellets into a semi-porous structure, seen in Fig. 7, at high hydrogenation levels at 294 K helps to increase the flow of molecular hydrogen to unreacted sites, and, thus, increases the hydrogen scavenging effects. But at 303 K, the getter pellets still looked partially liquefied at the end of the hydrogen uptake experiment, suggesting the lack of a complete re-solidification process and therefore the absence of a surge in the getter performance near the getter's end of life at a temperature just a few degrees above 294 K. Unfortunately, further in-depth studies into the liquefaction of DPB getter pellets upon hydrogenation and subsequent re-solidification at high hydrogenation levels as a function of temperature are beyond the scope of this work.

Overall, even though the predictive models presented in Figs. 12 and 13 do not fit the experimental hydrogen pressure rise data precisely, they successfully exhibit the trends of the hydrogen pressure buildup and serve to give reasonable predictions of the rate dependence on the getter pellets' consumed capacity. With that in mind, this semi-empirical kinetic prediction model can be used to predict the hydrogen pressure buildup in many practical device applications. For example, in Fig. 14, the hydrogen pressure buildup over more than a decade in a device having a free volume of 1000 cc, containing 300 DPB pellets, and subjected to a constant hydrogen input rate of 100 standard cubic centimeters per year (sccy) is presented. In this plot, the solid line and the dashed line represent the hydrogen pressure in the same device at 294 K and 303 K, respectively. Within experimental errors, the hydrogen pressure buildup seems to grow rapidly at both temperatures after about 33–40% consumed capacity. Even though the performance of the DPB getter does not reach its lowest level until beyond 60% hydrogenation level (see Figs. 9(b) and 13(a)), it seems to be a safe practice to replace the DPB getter pellets after about 33–40% consumed capacity when the hydrogen pressure starts to increase rapidly. Note that due to the dependence of the DPB getter pellets' performance on temperature and the semi-empirical nature of the hydrogen uptake prediction model presented in this report, predictive modeling of the getter pellets' performance at temperature outside the range of 294–303 K presented in this work should be based on data taken in the proper temperature range and analyzed in a similar manner.

4. Summary and discussion

4.1. Summary

The physical and chemical properties of DPB getter pellets during hydrogenation were examined. The hydrogen uptake kinetics of these getter pellets were measured with a thermogravimetric analyzer (TGA) under isothermal, isobaric conditions at higher hydrogen partial pressure. The kinetics obtained was then used

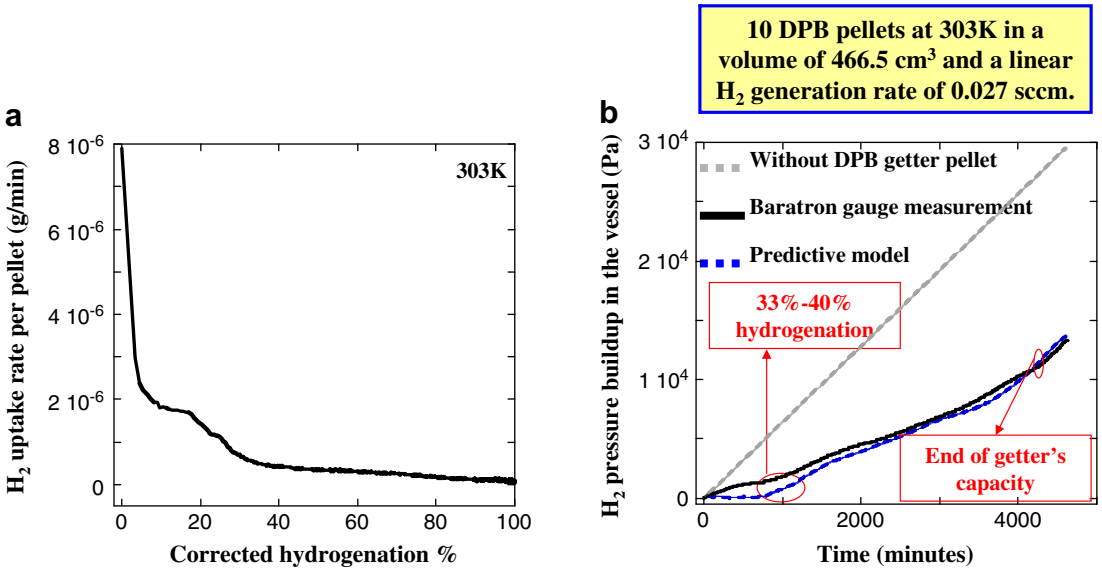

Fig. 13. (a) The weight gain rate per pellet vs. corrected hydrogenation percentage curve for a typical experiment with DPB pellets at 303 K in an isobaric environment of one atmosphere (10% H_2 + 90% He); (b) Hydrogen pressure in a vacuum vessels having a free volume of 466.5 cc without DPB getter pellets (light dashed lines) and with 10 DPB getter pellets (dark solid lines) at 303 K under a constant hydrogen input rate of 0.027 sccm. The dark dashed line represents the hydrogen pressure rise as predicted by the semi-empirical kinetic predictive model described in Eq. (5).

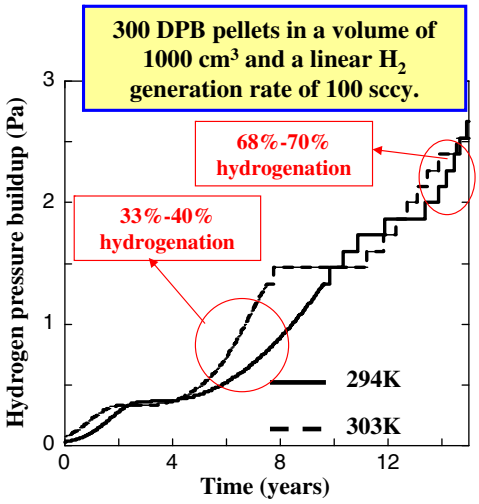

Fig. 14. Hydrogen pressure in a device having a free volume of 1000 cc, containing 300 DPB pellets, and subjected to a constant hydrogen input rate of 100 sccy.

to develop a semi-empirical model, based on gas diffusion into solids, to predict the hydrogen uptake under dynamic conditions and at lower hydrogen partial pressures. The predictive models were compared against independent experimental data on hydrogen pressure buildup in sealed systems containing DPB getter pellets and subjected to constant rates of hydrogen input. The equilibrium vapor pressures and volatility of the hydrogenated DPB products and their effects on the hydrogen uptake kinetics were also included in the predictive models. Due to the non-uniformity in the composition of the DPB getter pellets and experimental variability, the hydrogen uptake predictive models developed here do not fit precisely the independent data against which the models were validated. The models, however, successfully serve to give reasonable predictions of the dependence of the performance of the DPB getter pellets on their consumed capacity level, the instantaneous hydrogen partial pressure, the number of DPB getter pellets, and the free volume of the device. This investigation also reveals that the DPB getter pellets' performance drops significantly at ambient temperatures after the consumption of ~33–40% of the gettering capacity and that the pellets should probably be considered for replacement at this point. Nevertheless, in most practical devices equipped with plenty of DPB getter pellets, the hydrogen pressure buildup can be kept at safe levels for many years or even decades before this alarming point in the consumed capacity of the getters is reached. The methodology employed in developing the semi-empirical kinetic prediction approach presented here can also be used as a template for construction of kinetic prediction capability of gas uptake in other types of getters having complicated geometries and involving complex gas transport as long as the rate limiting step for the gas uptake is gas diffusion into a solid or liquid.

4.2. Discussion

Except for the lowest hydrogenation level (first few percents), similar behavior in the performance of DPB getter pellets as a function of hydrogenation (see Figs. 9(b) and 13(a)) has been reported in Ref. 4. At the lowest hydrogenation level, the H_2 gettering rates presented in Figs. 9(a) and 13(b) started out at their respective maximum rates then slowed down with further hydrogen uptake. On the contrary, the hydrogen uptake at the onset of the hydrogenation process in the gas-burette technique reported in Ref. 4 started out a factor of 10 or so slower than the maximum hydrogenation rate, increased to the maximum rate after a little more hydrogenation, then decreased with further hydrogenation. The temperature in the gas-burette experiments in Ref. 4 was kept at 290 K with a hydrogen pressure in the range of 0.1–100 Pa. For the isobaric isothermal experiments described in this report, the temperature was in the range of 294–303 K with a partial hydrogen pressure in excess of 10 000 Pa. Since temperature has been shown to drastically alter the uptake behavior near the end of life of DPB getter pellets (Figs. 9(b) and 13(a)) in the Results section above, it might also impact the performance of the getter at low hydrogenation level. From the Results section and based on the principles of gas diffusion into a solid/liquid, predictive modeling of the hydrogen uptake of the DPB pellets, at any particular temperature of interest, can be derived from isothermal isobaric

hydrogen uptake data taken at the same temperature, but at a higher hydrogen partial pressure and with order of magnitude accuracy (see Figs. 12 and 13). Ref. 4 also suggested the possibility of reproducing the hydrogen uptake rate vs. reaction extent curves at 100 Pa, 1 Pa, or 0.1 Pa by shifting the whole corresponding curve at 10 Pa up or down by some constant rates, confirming the validity of the principles of gas diffusion into a solid/liquid as the rate limiting step in the hydrogen uptake of DPB pellets, at least in a narrow pressure range of 0.1 Pa to 100 Pa. However, the differences in the trends of the uptake rates at low hydrogenation level between Ref. 4 and those presented in this work might be due not only to temperature differences, but also on the great differences in the hydrogen pressure regimes employed in the two sets of experiments. The discrepancies between the predicted uptake curves and actual hydrogen uptake curves shown in Figs. 12 and 13 confirm both the possibility and the risk in extrapolating kinetic data obtained in an isothermal isobaric condition at very high hydrogen pressure to a dynamic condition at a much lower pressure. In general, the accuracy of the semi-empirical hydrogen uptake prediction modeling illustrated in this report is at its best when the hydrogen uptake kinetic data employed in the semi-empirical modeling is obtained at a temperature and a pressure as close to their expected values in the intended application as practically possible.

Appendix A

Proof of $P_1t_1 = P_2t_2$ at the same value of conversion level and temperature for isothermal isobaric processes involving the diffusion and incorporation of a gas into a solid (or similarly in the case of liquid) as the rate limiting step.

A.1. The diffusion length vs. time curve is independent of surface curvature

Part I: The diffusion length vs. time curve is independent of surface curvature.

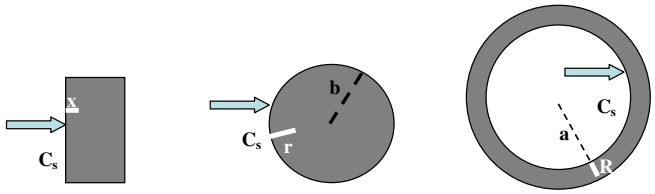

Diffusion into a slab | **Radial diffusion into a circular cylinder** | **Diffusion out of a hollow sphere**

A.1.1. For diffusion into a slab (one dimensional or 1D)

$$\text{From Fick's law of diffusion}: J = -D\nabla \cdot C = -\frac{DC_s}{x} \tag{Ia}$$

Here J is the diffusion flux, D is the diffusion coefficient, and C is the concentration of the diffusing species. C_s and x are the concentration of the diffusing gas at the surface of the slab facing the gas flow and the diffusing length, respectively.

Taking the point of view that diffusion involves the incorporation of the gaseous molecules into the slab matrix, J can also be written as

$$J = -\frac{1}{A}\frac{1}{m}\left(\rho A\frac{\mathrm{d}x}{\mathrm{d}t}\right) \tag{IIa}$$

Here A is the surface area of the slab which is perpendicular to the flow of gas and ρ is the density of the diffusing gas in the reacted layer. The mass of each molecule in the diffusing gas is labeled as m.

$$\text{Equate(Ia)and(Ib)to obtain}: x = \sqrt{2DC_s\frac{m}{\rho}t} \tag{IIIa}$$

A.1.2. For radial diffusion into a right circular cylinder (two dimensional or 2D)

Analogous to the case of gaseous diffusion into a slab:

$$J = -\frac{DC_s}{r} = -\frac{1}{2\pi(b-r)h}\frac{1}{m}\frac{\partial W_r}{\partial t} \tag{Ib}$$

Here r, b, and h are the radial diffusion length, the radius, and the height of the right circular cylinder, respectively. W_r is the weight gain due to the incorporation of the gas molecules into the reacted layer at the diffusion length r, and $\frac{\partial W_r}{\partial t}$ is the partial derivative of the weight gain with respect to time. Note that W_r is a function of both r and t

$$\text{But,}\frac{\partial W_r}{\partial t} = \rho\frac{\partial V_r}{\partial t} = \rho\frac{\partial V_r}{\partial r}\frac{\partial r}{\partial t} = \rho\left[2\pi(b-r)h\frac{\partial r}{\partial t}\right] \tag{IIb}$$

In Eq. (IIb), V_r is the volume of the reacted product layer. Equate (Ib) and (IIb) to obtain:

$$r = \sqrt{2DC_s\frac{m}{\rho}t} \tag{IIIb}$$

A.1.3. For diffusion out of a hollow sphere (three dimensional or 3D)

Analogous to the case above:

$$J = -\frac{DC_s}{R} = -\frac{1}{4\pi(a+R)^2}\frac{1}{m}\frac{\partial W_R}{\partial t} \tag{Ic}$$

In Eq. (Ic), a is the inner radius of the hollow sphere while R and W_R are the radial diffusion length and the weight gain due to the incorporation of the gas molecules into the reacted layer at R. Note that W_R is a function of both R and t

$$\text{But,}\frac{\mathrm{d}W_R}{\mathrm{d}t} = \rho\frac{\partial V_R}{\partial t} = \rho\frac{\partial V_R}{\partial R}\frac{\partial R}{\partial t} = \rho\left[\frac{4}{3}\pi(3a^2+6aR+3R^2)\frac{\partial R}{\partial t}\right] \tag{IIc}$$

In equation (IIc), V_R is the volume of the reacted product layer. Equate (Ic) and (IIc) to obtain:

$$R = \sqrt{2DC_s\frac{m}{\rho}t} \tag{IIIc}$$

The diffusion length vs. time curves for other diffusion geometries can also be analogously obtained. A comparison of Eqs. (IIIa), (IIIb), and (IIIc) reveals that the values of the diffusion length as a function of time are identical and independent of the surface curvature or the 1D, 2D or 3D nature of the diffusion process if the concentration of the diffusing species at the surface perpendicular to the gas flow (C_s) is the same.

A.2. Proof of $P_1t_1 = P_2t_2$ at the same value of conversion level and temperature for isothermal, isobaric processes involving the diffusion of a gas into a solid (or similarly in the case of liquid) as the rate limiting step

A.2.1. For diffusion into a slab (1D)

A specific conversion level (or hydrogenation level as in the case of hydrogen uptake by getters) corresponds with a specific weight gain $W = \rho Ax$ due to the incorporation of the gaseous molecules into the host matrix. So, if the experiment is carried out at a constant pressure P_1, then from Eq. (IIIa):

$$W = \rho A\sqrt{2DC_s(T,P_1)\frac{m}{\rho}t_1} \tag{IVa}$$

Similarly, if the experiment is done at a constant pressure P_2:

$$W = \rho A\sqrt{2DC_s(T,P_2)\frac{m}{\rho}t_2} \tag{Va}$$

For gas diffusion into a solid, the concentration of the diffusing species at the surface of the sample perpendicular to the flow of gas is directly proportional to the partial pressure of the diffusing species so that: $C_s(T,P_1) \propto P_1$ and $C_s(T,P_2) \propto P_2$. Substitute these values into equations (IVa) and (Va) and divide (IVa) by (Va) to see:

$$1 = \frac{\sqrt{P_1 t_1}}{\sqrt{P_2 t_2}} \tag{VIa}$$

Or $P_1 t_1 = P_2 t_2$ for a given weight gain at a given temperature.

A.2.2. For radial diffusion into a right circular cylinder (2D)

At a specific conversion level or weight gain W, $W = \rho V$ where V is the volume of the reacted product layer. If the experiment is performed at pressure P_1:

$$W = \rho h\pi[b^2 - \{b - r(T,P_1,t_1)\}^2] \tag{IVb}$$

If the experiment is done at pressure P_2:

$$W = \rho h\pi[b^2 - \{b - r(T,P_2,t_2)\}^2] \tag{Vb}$$

$$\text{From equations (IVb) and (Vb)}: r(T,P_1,t_1) = r(T,P_2,t_2) \tag{VIb}$$

For the same reason as in the case of diffusion into a slab: $C_s(T,P_1) \propto P_1$ and $C_s(T,P_2) \propto P_2$. With this and Eq. (IIIb), the relationship (VIb) can be rearranged to read: $\sqrt{P_1 t_1} = \sqrt{P_2 t_2}$ or $P_1 t_1 = P_2 t_2$ for a given weight gain at a given temperature.

A.2.3. For diffusion out of a hollow sphere (3D)

Perform analogous analysis as in the case of radial diffusion into a right circular cylinder to see: $W = \rho\frac{4}{3}\pi[\{a + R(T,P_1,t_1)\}^3 - a^3] = \rho\frac{4}{3}\pi[\{a + R(T,P_2,t_2)\}^3 - a^3]$

So: $R(T,P_1,t_1) = R(T,P_2,t_2)$ and $P_1 t_1 = P_2 t_2$ for a given weight gain at a given temperature.

Analogous analysis can also be used to arrive at the same conclusion for other geometries.

Appendix B

B.1. Derivation of Eq. (5)

The hydrogen partial pressure in a device, P, is a function of both time, t, and the hydrogenation percentage or consumption level of the DPB pellets, α, and can be written as

$$P(t,\alpha) = P(t - \Delta t, \alpha - \Delta\alpha) + \Delta P_D - \Delta P_G \tag{VII}$$

The meaning of Eq. (VII) is that the hydrogen partial pressure in the device, $P(t,\alpha)$, is simply equal to the hydrogen partial pressure at an earlier time, $t-\Delta t$, when the consumption level of the getter pellets is $\alpha-\Delta\alpha$, plus the hydrogen pressure increase due to all hydrogen generating processes in the device (ΔP_D) during the time Δt minus the hydrogen pressure decrease due to the hydrogen scavenging effect of the DPB pellets (ΔP_G) during that same time interval.

If the free volume of a device is V and the mole of hydrogen captured by N pellets of DPB is n, then from the ideal gas law:

$$V\frac{\Delta P_G}{\Delta t} = RT\frac{\Delta n}{\Delta t} = \frac{RT}{M_{H_2}}\left(N\frac{\Delta W}{\Delta t}\right) \tag{VIII}$$

In Eq. (VIII), R is the molar gas constant, M_{H_2} is the molecular weight of hydrogen, $\frac{\Delta P_G}{\Delta t}$ is the rate of hydrogen pressure decrease due to the scavenging action of the DPB getter pellets, and $\frac{\Delta W}{\Delta t}$ is the rate of weight gain due to hydrogen uptake of just one DPB pellet.

If the temperature involved in two isothermal, isobaric hydrogen uptake experiments at pressure P_1 and pressure P_2 are the same, then at any specific weight gain W and from Eq. (4):

$$\frac{P_2}{P_1} = \frac{t_1}{t_2} = \frac{Wt_1}{Wt_2} = \frac{W/t_2}{W/t_1} \tag{IX}$$

Realizing that, for isobaric experiments, P_2/P_1 is just a constant at all values of W, t_2, and t_1, Eq. (IX) can be rewritten as

$$\frac{t_1}{t_2} = \frac{P_2}{P_1} = \frac{\Delta W/\Delta t_2}{\Delta W/\Delta t_1} \tag{X}$$

Note that $\Delta W/\Delta t_1$ is simply the rate of weight gain under the isothermal, isobaric condition at T and higher pressure P_1 and can be relabeled as $\Delta W_E/\Delta t$ if P_1 is relabeled as P_E. Similarly, $\Delta W/\Delta t_2$ is simply the rate of weight gain under the isothermal, isobaric condition at T and lower pressure P_2 and can be relabeled as $\Delta W/\Delta t$ if P_2 is relabeled as P. With the above changes in symbols, Eq. (X) becomes:

$$\frac{\Delta W}{\Delta t} = \frac{P}{P_E}\frac{\Delta W_E}{\Delta t} \tag{XI}$$

Substitute Eq. (XI) into Eq. (VIII) to see:

$$\frac{\Delta P_G}{\Delta t} = \frac{NRT}{VM_{H_2}}\frac{P}{P_E}\frac{\Delta W_E}{\Delta t} \tag{XII}$$

Note that the hydrogen partial pressure P in a real device is not constant over a long period of time. However, if the unit of time is chosen to be very small, such as $\Delta t = 1$ s, then during each Δt interval, the condition of constant pressure can be practically assumed and the use of Eq. (4) and Eq. (XII) during each Δt interval is justified. Also with $\Delta t = 1$ s in a numerical calculation, the difference in $P(t, \alpha)$ and $P(t-\Delta t, \alpha-\Delta\alpha)$ is negligible and Eq. (XII) can be approximated by

$$\frac{\Delta P_G}{\Delta t} \approx \frac{NRT}{VM_{H_2}}\frac{P(t-\Delta t, \alpha-\Delta\alpha)}{P_E}\frac{\Delta W_E}{\Delta t} \tag{XIII}$$

Since $\Delta W_E/\Delta t$ was obtained experimentally as a function of hydrogenation percentage α (see Fig. 9(b) and 13 (b) and Appendix C), it is logical to replace $\frac{\Delta W_E}{\Delta t}$ with $W'_E(\alpha)$ in Eq. (XIII):

$$\frac{\Delta P_G}{\Delta t} \approx \frac{NRT}{VM_{H_2}}\frac{P(t-\Delta t, \alpha-\Delta\alpha)}{P_E}W'_E(\alpha) \tag{XIV}$$

Note that in this work, the hydrogen generation processes in the device, P_D, is independent of the hydrogen pressure buildup in the system and of the hydrogenation percentage of the DPB pellets ($P'_D \equiv \frac{\Delta P_D}{\Delta t}$ is only a constant or a function of time). Substitute Eq. (XIV) into Eq. (VII) to see:

$$P(t,\alpha) = P(t-\Delta t, \alpha-\Delta\alpha) + P'_D(t)\Delta t - \frac{NRT}{VM_{H_2}} \times \frac{P(t-\Delta t, \alpha-\Delta\alpha)}{P_E}W'_E(\alpha)\mathrm{d}t \tag{XV}$$

Due to the volatility of hydrogenated DPB, hydrogenated DPB vapor continues to build in the device until an equilibrium vapor pressure (see Eq. (2), Table 1, Figs. 2 and 3) is reached in the device. In order to properly account for this volatility, $\frac{P(t-\Delta t,\alpha-\alpha)}{P_E}W'_E(\alpha)$ in Eq. (XV) needs to be modified to read:

$$\frac{P(t-\Delta t, \alpha-\Delta\alpha)}{P_E}W'_E(\alpha) - \left[W'_L(\alpha)\frac{P_{\mathrm{equi}}(T)}{P_{\mathrm{equi}}(294\mathrm{K})}\right]\frac{P_{\mathrm{equi}}(T) - P_a(t-\Delta t, \alpha-\Delta\alpha)}{P_{\mathrm{equi}}(T)} \tag{XVI}$$

Here, $W'_L(\alpha)$ is the experimentally obtained rate of weight loss of just one DPB pellet as a function α at 294 K (see Fig. 8 and Appendix C), $P_{\mathrm{equi}}(T)$ is the equilibrium vapor pressure of the hydrogenated

product at temperature T, and $P_a(t-\Delta t, \alpha-\Delta\alpha)$ is the actual vapor pressure of the hydrogenated product in the device at time $t-\Delta t$ and hydrogenation level $\alpha-\Delta\alpha$. When P_a reaches its theoretical maximum which is the value of P_{equi}, the vaporization of the hydrogenated product stops and the second term in Eq. (XVI) vanishes thereafter, P_a can be obtained from:

$$P_a(t-\Delta t, \alpha-\Delta\alpha) = \left[\frac{\sum_{i=1}^{(t-\Delta t)/\Delta t} W'_L(\alpha)\Delta t_i}{M_{\text{hydrogenated DPB}}}\right]\left(\frac{RT}{V}\right) \quad \text{(XVII)}$$

With the modification of W'_E presented in Eq. (XVI), Eq. (XV) becomes:

$$P(t,\alpha) = P(t-\Delta t, \alpha-\Delta\alpha) + P'_D(t)\Delta t - \left(\frac{NRT}{VM_{H_2}}\right) \times \left\{\frac{P(t-\Delta t,\alpha-\Delta\alpha)}{P_E} W'_E(\alpha) - \left[W'_L(\alpha)\frac{P_{equi}(T)}{P_{equi}(294K)}\right]\frac{P_{equi}(T)-P_a(t-\Delta t,\alpha-\Delta\alpha)}{P_{equi}(T)}\right\}\Delta t$$

This is Eq. (5) with α determined by

$$\alpha = 100\frac{\left[\frac{\sum_{i=1}^{t/\Delta t}\left\{W'_E(\alpha) - \left[W'_L(\alpha)\frac{P_{equi}(T)}{P_{equi}(294K)}\right]\frac{P_{equi}(T)-P_a(t-\Delta t,\alpha-\Delta\alpha)}{P_{equi}(T)}\right\}\Delta t_i}{0.75m_p}\right]}{(4M_{H_2}/M_{DPB})} \quad \text{(XIX)}$$

In formula (XIX), m_p is the mass of one virgin DPB pellet which is roughly 0.020562 g, M_{DPB} is the molecular weight of DPB which is 202 g/mol, and M_{H_2} is the molar weight of hydrogen which is 2 g/mol.Note that α as defined in Eq. (XIX) is the argument in the $W'_E(\alpha)$ and $W'_L(\alpha)$ formulae, and accounts for the dependence of the weight gain and weight loss in a device with a dynamic hydrogen pressure on the volatility of the hydrogenated product. The absolute hydrogenation percentage of the DPB getter pellets in a dynamic hydrogen pressure situation, α_a is simply given by

$$\alpha_a = 100\frac{\left[\frac{\sum_{i=1}^{t/\Delta t} W'_E(\alpha)\Delta t_i}{0.75m_p}\right]}{(4M_{H_2}/M_{DPB})} \quad \text{(XX)}$$

Appendix C

C.1. Expressions for W'_E vs. α at 294 K and 303 K, and for W'_L vs. α at 294 K

C.1.1. fit of the weight loss rate vs. apparent hydrogenation percentage curve of Fig. 8

The weight loss rate vs. apparent hydrogenation percentage curve in Fig. 8 can be fitted with any suitable mathematical formulation. A combination of a log normal distribution and a polynomial in a double precision format (16 digits) is a suitable analog fit to such a curve and can be expressed as

$$y = \frac{1}{60.0}\left\{(1.821532826222945\times10^{-6})\frac{\exp\left(-\frac{(\ln x-2.894902118339475)^2}{2(0.3206153397880946)^2}\right)}{0.3206153397880946(\sqrt{2\pi})x}\right\} + (3.209230033600553\times10^{-9}) + (8.894459295108791\times10^{-10})x + (1.802929976313459\times10^{-10})x^2 - (7.142718159120020\times10^{-12})x^3 + (8.754141192227882\times10^{-14})x^4 - (3.482304837056636\times10^{-16})x^5$$

where y represents the weight loss rate, W'_L, in unit of g/s at 294 K and x is apparent hydrogenation percentage.

C.1.2. Fit of the weight gain rate vs. hydrogenation percentage curve at 294 K (Fig. 9(b))

Due to the peak around 85% hydrogenation, the curve should be broken into two parts for separate fittings. The portion of the curve up to 85% hydrogenation percentage can be fitted with a polynomial of 9th order as following:

$$y = (1.781749263701982e^{-5} - 4.35974684650211e^{-6}x + 4.867236167211415e^{-7}x^2 - 2.967803500300019e^{-8}x^3 + 1.094432541422219e^{-9}x^4 - 2.560257404971820e^{-11}x^5 + 3.830285181462341e^{-13}x^6 - 3.552048562863368e^{-15}x^7 + 1.859176702897421e^{-17}x^8 - 4.195181533490433e^{-20}x^9) \times \frac{1}{60.0}$$

where y is the weight gain rate, W'_E, in unit of gram per minute (g/min) and x is hydrogenation percentage [corrected or absolute hydrogenation percentage in the case of an isothermal, isobaric experiment as presented in Fig. 9(b), but an apparent hydrogenation percentage in the case of a dynamic hydrogen pressure situation like that in a device kinetic prediction].

The portion of the curve beyond 85% hydrogenation percentage can be fitted with a polynomial of 3th order as following:

$$y = 0.01308060344426399 - 0.0004459376177877662x + 5.061855532282121e^{-6}x^2 - 1.912834748097113e^{-8}x^3$$

with y and x defined as above.

C.1.3. Expression of the weight gain rate vs. hydrogenation percentage curve at 303 K (Fig. 13(a))

The curve can be satisfactorily fitted with a polynomial of 9th order as following:

$$y = 7.570930727541158e^{-6} - 1.866004587105619e^{-6}x + 2.348796534139313e^{-7}x^2 - 1.521736701486185e^{-8}x^3 + 5.601249720088819e^{-10}x^4 - 1.246256159712781e^{-11}x^5 + 1.711439625409121e^{-13}x^6 - 1.420023916007660e^{-15}x^7 + 6.530460222687018e^{-18}x^8 - 1.278537085586561e^{-20}x^9$$

With y and x defined as in the case at 294 K.

References

[1] S. Yamanaka, Y. Sato, A. Ogawa, Y. Shirasu, M. Miyake, J. Nucl. Mater. 179 (1991) 303.
[2] S. Bredendiekamper, H. Kleweneherius, G. Pfennig, M. Bruns, M. Deviller, H.J. Ache, Z. Prenius, Anal. Chem. 335 (1989) 669.
[3] M. Balooch, Wei-E Wang, J.R. Kirkpatrick, J. Polym. Sci. B 39 (2001) 425.
[4] G.L. Powell, J. Alloys Compd. 446–447 (2007) 402.
[5] G.L. Powell, Advanced Materials for Energy Conversion II Symposium, TMS, 2004, p. 467.
[6] G.L. Powell, Advanced Materials for Energy Conversion II Symposium, TMS, 2004, p. 257.
[7] A. Maiti, R.H. Gee, R. Maxwell, A.P. Saab, Chem. Phys. Lett. 440 (2007) 244.
[8] J.C. Weigle, J. Phillips, AIChE J. 50 (2004) 821.